

# Multiple Ionization Mass Spectrometry Strategy Used To Reveal the Complexity of Metabolomics

Anders Nordström,<sup>\*,†,‡</sup> Elizabeth Want,<sup>†,§</sup> Trent Northen,<sup>†</sup> Janne Lehtiö,<sup>‡</sup> and Gary Siuzdak

Department of Molecular Biology and The Center for Mass Spectrometry, The Scripps Research Institute, 10550 North Torrey Pines Road, La Jolla California 92037, and Karolinska Biomics Center, Z5:02, Karolinska Institutet and Karolinska University Hospital, SE-171 76, Stockholm, Sweden

A multiple ionization mass spectrometry strategy is presented based on the analysis of human serum extracts. Chromatographic separation was interfaced inline with the atmospheric pressure ionization techniques electrospray ionization (ESI) and atmospheric pressure chemical ionization (APCI) in both positive (+) and negative (−) ionization modes. Furthermore, surface-based matrix-assisted laser desorption/ionization (MALDI) and desorption ionization on silicon (DIOS) mass spectrometry were also integrated with the separation through fraction collection and offline mass spectrometry. Processing of raw data using the XCMS software resulted in time-aligned ion features, which are defined as a unique  $m/z$  at a unique retention time. The ion feature lists obtained through LC–MS with ESI and APCI interfaces in both  $\pm$  ionization modes were compared, and unique ion tables were generated. Nonredundant, unique ion features, were defined as mass numbers for which no mass numbers corresponding to  $[M + H]^+$ ,  $[M - H]^-$ , or  $[M + Na]^+$  were observed in the other ionization methods at the same retention time. Analysis of the extracted serum using ESI for both (+) and (−) ions resulted in >90% additional unique ions being detected in the (−) ESI mode. Complementing the ESI analysis with APCI resulted in an additional ~20% increase in unique ions. Finally, ESI/APCI ionization was combined with fraction collection and offline-MALDI and DIOS mass spectrometry. The parts of the total ion current chromatograms in the LC–MS acquired data corresponding to collected fractions were summed, and  $m/z$  lists were compiled and compared to the  $m/z$  lists obtained from the DIOS/MALDI spectra. It was observed that, for each fraction, DIOS accounted for ~50% of the unique ions detected. These results suggest that true global metabolomics will require multiple ionization technologies to address the inherent metabolite diversity and therefore the complexity in and of metabolomics studies.

Quantitative global analysis of endogenous metabolites from cells, tissues, fluids or whole organisms—metabolomics—is becoming an integral part of functional genomics efforts<sup>1–3</sup> as well as a tool for finding diagnostic biomarkers.<sup>4–7</sup> From a mass spectrometry ionization point of view, the transcriptome and proteome are relatively homogeneous in their respective physical–chemical composition of 4 and 20 chemical building blocks, whereas vast physical–chemical heterogeneity is contained in the metabolome, where the complexity is dictated at the atomic level presenting diversity similar to that of combinatorial libraries. This diversity makes it especially challenging to gain a comprehensive and quantitative measure of the metabolome. For example, simultaneous separation and mass spectrometric detection of the substrate–product pair fructose and fructose 1-phosphate is not trivial.

Nuclear magnetic resonance spectroscopy (NMR)<sup>8</sup> and mass spectrometry (MS)<sup>9,10</sup> have become the primary analytical technologies of metabolomics, where they have a great potential to complement each other.<sup>11</sup> Theoretically, <sup>1</sup>H and <sup>13</sup>C NMR are capable of measuring most aspects of the metabolome, yet the low concentrations (<pM) and the extremely large dynamic range (low abundant signaling compounds to central metabolism carbohydrates), typically encountered in biological systems paired

- (1) Fiehn, O.; Kopka, J.; Dormann, P.; Altmann, T.; Trethewey, R. N.; Willmitzer, L. *Nat. Biotechnol.* **2000**, *18*, 1157–1161.
- (2) Clish, C. B.; Davidov, E.; Oresic, M.; Plasterer, T. N.; Lavine, G.; Londo, T.; Meys, M.; Snell, P.; Stochaj, W.; Adourian, A.; Zhang, X.; Morel, N.; Neumann, E.; Verheij, E.; Vogels, J. T.; Havekes, L. M.; Afeyan, N.; Regnier, F.; van der Greef, J.; Naylor, S. *Omic* **2004**, *8*, 3–13.
- (3) Goodacre, R.; Vaidyanathan, S.; Dunn, W. B.; Harrigan, G. G.; Kell, D. B. *Trends Biotechnol.* **2004**, *22*, 245–252.
- (4) Brindle, J. T.; Antti, H.; Holmes, E.; Tranter, G.; Nicholson, J. K.; Bethell, H. W.; Clarke, S.; Schofield, P. M.; McKilligin, E.; Mosedale, D. E.; Grainger, D. J. *Nat. Med.* **2002**, *8*, 1439–1444.
- (5) Sabatine, M. S.; Liu, E.; Morrow, D. A.; Heller, E.; McCarroll, R.; Wiegand, R.; Berriz, G. F.; Roth, F. P.; Gerszten, R. E. *Circulation* **2005**, *112*, 3868–3875.
- (6) Kawashima, H.; Oguchi, M.; Ioi, H.; Amaha, M.; Yamanaka, G.; Kashiwagi, Y.; Takekuma, K.; Yamazaki, Y.; Hoshika, A.; Watanabe, Y. *Int. J. Neurosci.* **2006**, *116*, 927–936.
- (7) Ippolito, J. E.; Xu, J.; Jain, S.; Moulder, K.; Mennerick, S.; Crowley, J. R.; Townsend, R. R.; Gordon, J. I. *Proc. Natl. Acad. Sci. U.S.A.* **2005**, *102*, 9901–9906.
- (8) Griffin, J. L. *Curr. Opin. Chem. Biol.* **2003**, *7*, 648–654.
- (9) Want, E. J.; Nordstrom, A.; Morita, H.; Siuzdak, G. *J. Proteome Res.* **2007**, *6*, 459–468.
- (10) Villas-Boas, S. G.; Mas, S.; Akesson, M.; Smedsgaard, J.; Nielsen, J. *Mass Spectrom. Rev.* **2005**, *24*, 613–646.
- (11) Sandvoss, M.; Weltring, A.; Preiss, A.; Levsen, K.; Wuensch, G. *J. Chromatogr., A* **2001**, *917*, 75–86.

\* To whom correspondence should be addressed. E-mail: anders.nordstrom@ki.se.

<sup>†</sup> The Scripps Research Institute.

<sup>‡</sup> Karolinska Institutet and Karolinska University Hospital.

<sup>§</sup> Present address: Biomolecular Medicine, Division of Surgery, Oncology, Reproductive Biology and Anaesthetics, Sir Alexander Fleming Building, Imperial College, London SW7 2AZ, UK.

with difficulties in coupling NMR to chromatography, put some restrictions on NMR as a tool for initial data acquisition in metabolomics since important aspects of the metabolome composition potentially pass unmeasured. Mass spectrometry offers very high sensitivity and a good dynamic range through its measurement of an analyte as a charged molecule.

The experimental aim in global metabolomics studies is to obtain a comprehensive, quantitative, and unbiased view of the metabolome, and a key to this goal is the mass spectrometry ionization event. Several different ionization methods and mass spectrometry platforms have been probed in a metabolomics context such as electron impact ionization (EI),<sup>1,12–14</sup> electrospray ionization (ESI),<sup>15–18</sup> atmospheric pressure chemical ionization (APCI),<sup>19</sup> desorption electrospray ionization (DESI),<sup>20</sup> matrix-assisted laser desorption/ionization (MALDI),<sup>21</sup> and desorption/ionization on silicon (DIOS).<sup>22</sup> All of the above-mentioned ionization techniques discriminate differently and specifically/uni- quely against certain analyte physical–chemical properties. Here, the possibility of using a multiple ionization mode approach to mass spectrometry-based metabolomics was explored, motivated by the prospect of potentially detecting more metabolites through an extended mass spectrometry ionization strategy. Three levels of multimode ionization were tested: (I) acquisition of mass spectrometry data in both positive and negative mode; (II) combination of the two atmospheric pressure ionization techniques ESI and APCI as well as a simultaneous ESI/APCI ionization source<sup>23</sup> referred to as multimode ionization (MM); (III) combination of LC inline atmospheric pressure ionization techniques with LC fraction collection and offline MALDI/DIOS analysis. Our results reveal a large potential for an increase in the number of detected ion species through the use of multiple ionization, which at least in part can be translated into an increased coverage of the metabolome.

## METHODS

**Materials and Serum Extraction.** Solvents used were of HPLC grade. All metabolite standards were ordered in high purity from Sigma Aldrich (St. Louis, MO) except for the <sup>2</sup>H<sub>5</sub>-phenylalanine, which was obtained through Cambridge Isotope Laboratories (Andover, MA). All serum was human serum from clotted human male whole blood, sterile-filtered (Sigma). Protein pre-

cipitation of five aliquots (100  $\mu$ L) of the human serum was performed using a cold methanol method.<sup>15</sup> The extracted aliquots were dried, resuspended in 100  $\mu$ L of MeOH/2-propanol/acetone/H<sub>2</sub>O (2.5:1.25:1.25:95), and subsequently pooled and transferred to HPLC vials.

**LC–MS.** The extracted serum was analyzed using three different ionization modes: ESI, APCI, and simultaneous ESI/APCI (MM). Data were acquired in both positive (+) and negative (–) polarity for each ionization mode resulting in six different categories of LC–MS analysis. For each category, 5 replicate injections were performed resulting in a total of 30 injections. An LC-MSD SL system from Agilent (Santa Clara, CA), equipped with the Agilent multimode source (MM-source), was used for the LC–MS analysis. This ion source is capable of performing separate ESI/APCI ionization or a simultaneous ESI/APCI ionization, termed multimode ionization. Chromatographic separation was achieved on a Zorbax SB-C18 column (2.1  $\times$  150 mm, 3.5- $\mu$ m particle size, Agilent) with an injection volume of 5  $\mu$ L. The mobile phases were as follows: (A) H<sub>2</sub>O and (B) MeOH/2-propanol/acetone (50:25:25), with a flow rate of 200  $\mu$ L/minute. Gradient conditions were as follows: 0–2 min hold at 5% B, 2–25 min linear gradient 5%–95% B, 25–35 min hold at 95% B, 35–35.5 min 95–5%B, and 35.5–45 min hold at 5% B. The column was placed in a heater element set to 60  $^{\circ}$ C to reduce column back pressure caused by the rather large fraction (25%) of 2-propanol in mobile phase B. The mass range scanned was  $m/z$  100–1000 in full data storage mode. The estimated instrumental resolution is 1000 with data being generated at nominal mass accuracy. Ionization conditions were as follows: APCI, drying gas 12 L/min, nebulizing gas pressure 20 psig, drying gas temperature 350  $^{\circ}$ C, vaporizing temperature 250  $^{\circ}$ C, capillary 2000 V, corona current 5  $\mu$ A, and charging voltage 2000 V; ESI, drying gas 12 L/min, nebulizing gas pressure 60 psig, drying gas temperature 250  $^{\circ}$ C, vaporizing temperature 150  $^{\circ}$ C, capillary 2000 V, and charging voltage 2000 V; MM, drying gas 12 L/min, nebulizing gas pressure 40 psig, drying gas temperature 300  $^{\circ}$ C, vaporizing temperature 200  $^{\circ}$ C, capillary 2000 V, corona current 1  $\mu$ A, and charging voltage 2000 V. The same ionization parameters were kept when switching between  $\pm$  ionization.

**MALDI/DIOS.** The DIOS chips were prepared as described previously<sup>24</sup> with the following exceptions. Low-resistivity (0.01–0.02  $\Omega$ -cm) p-type (1–0-0) silicon wafers (500–550- $\mu$ m thickness) were used from Silicon Quest International (Santa Clara, CA). For the anodic etching process, a custom-made Teflon cell allowing for backside illumination was used. The silicon chips were placed on top of a gold foil (anode) with a square (2.5  $\times$  2.5 cm) cut out of it (area to be etched). A platinum wire (cathode) was placed in the cell cavity filled with 10 mL of 25% hydrofluoric acid in ethanol (v/v). The silicon wafer was subsequently electrochemically etched (15 min) with a current of 25 mA (cm<sup>2</sup>)<sup>–1</sup> under white light from a fiber-optic light source hosting a 250-W quartz/halogen lamp (model I-250, CUDA Fiberoptics). Oxidation and derivatization of the oxidized porous silicon surface was performed as previously described<sup>24</sup> after which the chip was fitted onto a modified MALDI target (Applied Biosystems) with an adhesive

- (12) Jellum, E. *J. Chromatogr.* **1977**, *143*, 427–462.
- (13) Jonsson, P.; Gullberg, J.; Nordstrom, A.; Kusano, M.; Kowalczyk, M.; Sjoström, M.; Moritz, T. *Anal. Chem.* **2004**, *76*, 1738–1745.
- (14) Kopka, J. *J. Biotechnol.* **2006**, *124*, 312–322.
- (15) Want, E. J.; O'Maille, G.; Smith, C. A.; Brandon, T. R.; Uritboonthai, W.; Qin, C.; Trauger, S. A.; Siuzdak, G. *Anal. Chem.* **2006**, *78*, 743–752.
- (16) Waybright, T. J.; Van, Q. N.; Muschik, G. M.; Conrads, T. P.; Veenstra, T. D.; Issaq, H. J. *J. Liq. Chromatogr. Relat. Technol.* **2006**, *29*, 2475–2497.
- (17) Tolstikov, V. V.; Lommen, A.; Nakanishi, K.; Tanaka, N.; Fiehn, O. *Anal. Chem.* **2003**, *75*, 6737–6740.
- (18) Nordstrom, A.; O'Maille, G.; Qin, C.; Siuzdak, G. *Anal. Chem.* **2006**, *78*, 3289–3295.
- (19) Aharoni, A.; Ric de Vos, C. H.; Verhoeven, H. A.; Maliepaard, C. A.; Kruppa, G.; Bino, R.; Goodenow, D. B. *Omic* **2002**, *6*, 217–234.
- (20) Chen, H.; Pan, Z.; Talaty, N.; Rafferty, D.; Cooks, R. G. *Rapid Commun. Mass Spectrom.* **2006**, *20*, 1577–1584.
- (21) Vaidyanathan, S.; Gaskell, S.; Goodacre, R. *Rapid Commun. Mass Spectrom.* **2006**, *20*, 1192–1198.
- (22) Vaidyanathan, S.; Jones, D.; Broadhurst, D. I.; Ellis, J.; Jenkins, T.; Dunn, W. B.; Hayes, A.; Burton, N.; Oliver, S. G.; Kell, D. B.; Goodacre, R. *Metabolomics* **2005**, *1*, 243–250.
- (23) Fisher, S. M.; Perkins, P. D. Agilent technical note, 2005.

- (24) Nordstrom, A.; Apon, J. V.; Uritboonthai, W.; Go, E. P.; Siuzdak, G. *Anal. Chem.* **2006**, *78*, 272–278.

**Table 1. Unique Ion Features in Positive and Negative Ionization Modes Detected in Human Blood Serum Extract**

ionization method and polarity	total no. of ion features	ion features with corresponding ions at same RT and $m/z$ (+2, +24 or -2, -24) in opposite polarity <sup>a</sup>	no. of unique ion features	unique ion features (%)
ESI (+)	512	28	484	95
ESI (-)	503	28	475	94
APCI (+)	265	6	259	98
APCI (-)	223	6	217	97
MM (+)	467	21	446	96
MM (-)	408	21	387	95

<sup>a</sup> For definition of unique positive/negative ions, see Increasing Metabolite Coverage. (I) Positive and Negative Ionization.

tape. WARNING! Extreme care should be taken when handling HF.

The serum extract was subject to LC separation and 10-min fractions (1 mL) were collected postcolumn by splitting flow 1:1 using a PEEK tee. The four fractions collected during the LC separation were dried down and resuspended for DIOS analysis in 100  $\mu$ L of 0.5 mM perfluorooctanesulfonic acid (Sigma) in 50:50 MeOH/H<sub>2</sub>O and in 100  $\mu$ L of 50:50 MeOH/H<sub>2</sub>O for MALDI analysis. From these solutions, 0.5  $\mu$ L was spotted on to the DIOS and MALDI chips, respectively. To the MALDI samples, 0.5  $\mu$ L of a 10 mg/mL 2,5-dihydroxybenzoic acid in 50:50 acetonitrile/H<sub>2</sub>O matrix solution was added. Each fraction was spotted three times, and three spectra were collected for each spot. All MALDI-DIOS-MS measurements were performed on an Applied Biosystems MALDI-TOF STR in the reflectron mode. The samples were irradiated with a 337-nm nitrogen laser operated at a repetition rate of 15 Hz. An acceleration voltage of 25 000 V was employed, and delayed extraction periods of 50–250 ns were used for optimal resolution. A laser energy setting of 1000 (arbitrary units) were used for all analyses. For the calibration curves, standard solutions each containing the four type compounds (Table 2) were prepared together with a fixed concentration of <sup>2</sup>H<sub>5</sub>-phenylalanine, the internal standard (IS) in the following molar ratios of standard/internal standard (S/IS): 0.2:1, 0.5:1, 1:1, 2:1, 3:1, and 5:1.

**Data Evaluation.** For ion feature generation and nonlinear retention time correction of the LC-MS data, we used the freely available XCMS<sup>25</sup> software. The LC-MS raw data files were converted to CDF format using Agilent's Data Analysis software and the 30 CDF files subsequently processed in one batch (six different folders, ESI-POS, ESI-NEG, APCI-POS, APCI-NEG, MM-POS, and MM-NEG by XCMS using default settings except for the XCMS processing parameters "missing" and "extra", which were both set to 25. The XCMS software identifies ion features (a specific  $m/z$  at a specific retention time), which subsequently are aligned with respect to the retention time across the analyzed samples. The ion features are reported in the format M340T1223, which would represent an ion with  $m/z$  340 at the retention time of 1223 s. For each sample, an intensity value is associated with the respective ion feature. Also associated with each ion feature is an  $m/z$  and retention time interval and median value in which

that specific ion feature was identified and the number of times a certain ion feature was identified within each sample class (ESI-POS, ESI-NEG, APCI-POS, APCI-NEG, MM-POS, MM-NEG).

**Reduction of Data Complexity.** The XCMS output was further processed using Microsoft Excel (Microsoft, Redmond, WA), using only ion features present between retention times 90 and 2580 s to reduce the complexity of the data. With the XCMS processing parameter "missing" set to 25, XCMS will report an ion feature in all processed samples if it is found in at least five of the samples. If no peak shape is found according to the Gaussian second-derivative criteria,<sup>25</sup> a baseline intensity will be reported. It was assumed that each feature reported was only detected in either positive or negative mode, and therefore, ion features were initially classified as being detected in positive or negative mode. For an ion feature to be assigned as "positive" or "negative", it had to be present in at least one of the five replicate analyses for that particular ionization mode/polarity. This was done by using the following Excel formula syntax on each ion feature row: =IF("cellref\_ESI-NEG">0,1,0) and subsequently changing the cell reference to the other five ionization modes/polarities. The term "cellref\_" in the rest of the text refers to a Microsoft Excel cell reference. Overall polarity classification, exemplified with "negative" classification, was then performed with following syntax applied to each ion feature row: =OR("cellref\_ESI-NEG">0,"cellref-APCI-NEG">0,"cellref-MM-NEG">0). The final sorting involved discarding all ion features with dual positive/negative assignments, since these were likely to be XCMS processing artifacts. The "positive" and "negative" ion feature lists were subsequently separately deisotoped in Microsoft Excel by pasting the ion feature lists together with the median  $m/z$  and retention time values associated with each ion feature. The list was then sorted according to ascending  $m/z$  value. All  $m/z$  and retention time values were subsequently subtracted from each other creating one " $m/z$ " subtraction matrix and one "retention time" subtraction matrix. With 901 ion features assigned as "positive" and 745 ion features assigned as "negative", these two matrices became 901  $\times$  901 cells in positive mode and 745  $\times$  745 cells in negative mode. If there for any given  $m/z$  value existed a  $m/z + 1$  value at the same retention time, the ion feature associated with the  $m/z + 1$  value was removed (deisotoped). To allow for a certain mass assignment error (data were acquired at unit mass resolution) and retention time assignment error, a  $m/z$  tolerance of  $\pm 0.2$  amu and a retention time tolerance of  $\pm 5$  s was allowed. The two subtraction matrices were subsequently queried simultaneously, cell by cell, with the following Excel formula syntax: =AND("cellref\_M/Z\_DIFF1">-1.2,"cellref\_M/Z\_DIFF1"<-0.8,"cellref\_RT\_DIFF1">-5,"cellref\_RT\_DIFF1"<5). The resulting TRUE/FALSE matrix of the same size as the two original subtraction matrices was subsequently queried cell by cell with the following syntax: =IF("cellref\_TRUE/FALSE1"=TRUE,"cellref\_ION-FEATURE2",0). This resulted in a list with ion features corresponding to the  $m/z + 1$  values previously identified; this list was used to filter out ion features corresponding to (+1) isotopes. The deisotoped positive ion feature list was used to create the Venn diagram by applying the previously described presence criteria (present in one of five replicates) on each ion feature row. This rather low stringency criterion was applied in order not to underestimate the redundancy of ions between the different

(25) Smith, C. A.; Want, E. J.; O'Maille, G.; Abagyan, R.; Siuzdak, G. *Anal. Chem.* **2006**, *78*, 779–787.



**Table 2. Linearity ( $R^2$ ) for Type Compound Calibration Curves<sup>a</sup> Using MALDI and DIOS**

	concentration range 2.5–12.5 $\mu\text{M}^a$				concentration range 2.5–62.5 $\mu\text{M}^a$			
	Phe <sup>b</sup>	Caf <sup>c</sup>	Chol <sup>d</sup>	malt <sup>e</sup>	Phe <sup>b</sup>	Caf <sup>c</sup>	Chol <sup>d</sup>	malt <sup>e</sup>
DIOS	0.977	0.999	0.987	0.999	0.938	0.875	0.697	0.817
MALDI	0.979	0.954	0.991	0.629	0.974	0.954	0.790	0.910

<sup>a</sup> Internal standard <sup>2</sup>H<sub>5</sub> phenylalanine used for all compounds ( $m/z$  171). <sup>b</sup> Phenylalanine ( $m/z$  166). <sup>c</sup> Caffeine ( $m/z$  195). <sup>d</sup> Cholesterol ( $m/z$  369). <sup>e</sup> Maltotriose ( $m/z$  527).

ionization modes ESI, APCI, and MM. The Venn diagram was created using the free Venn diagram generating resource at <http://www.venndiagram.tk>.

**Evaluation of Unique Ion Features.** To evaluate the number of unique ion features detected using ESI in positive and negative polarity, respectively, we removed all ion features in the “positive” ion feature list to which a corresponding ion feature in the “negative” list existed that represented an ion at  $-2$  or  $-24$  amu less. In this manner, a unique ion feature in positive mode was defined as a specific  $m/z$  ( $[\text{M} + \text{H}]^+$  or  $[\text{M} + \text{Na}]^+$ ) detected at a specific retention time for which there is no corresponding negative ion ( $[\text{M} - \text{H}]^-$ ) of the ion detected at the same retention time in negative mode. The mass and time tolerance was again set to  $\pm 0.2$  amu and  $\pm 5$  s. The same  $m/z$  and retention time subtraction matrices as for the deisotoping were calculated with values from the “positive” ion feature list being subtracted from the “negative” list. The resulting subtraction matrices were queried simultaneously with the following Excel formula syntax, =AND(“cellref\_M/Z\_DIFF1”>-2.2,“cellref\_M/Z\_DIFF1”<-1.8,“cellref\_RT\_DIFF1”>-5,“cellref\_RT\_DIFF1”<5), to find  $-2$  amu ion features and, =AND(“cellref\_M/Z\_DIFF1”>-24.2,“cellref\_M/Z\_DIFF1”<-23.8,“cellref\_RT\_DIFF1”>-5,“cellref\_RT\_DIFF1”<5) to find ion features at  $-24$  amu.

**Ionization Mode Comparison.** The ESI/APCI/DIOS/MALDI comparison was performed by exporting background-subtracted spectra summed over time segments corresponding to the fractions collected in ESI and APCI analysis. These spectra were subsequently filtered to contain only  $m/z$  values with at least 3% relative intensity. The  $m/z$  values above 3% relative intensity from MALDI and DIOS spectra were also exported, and  $m/z$  values that appeared in more than two of the fractions were eliminated as background ions, to compensate for the fact that the elution of a certain analyte might split in to two fractions but not three fractions. Also a particular  $m/z$  had to be present in more than five of the nine spectra acquired with DIOS and MALDI. (chosen with respect to ionization reproducibility). Since the  $m/z$  lists were generated from both high-resolution data (DIOS/MALDI) and nominal mass data (ESI/APCI), the  $m/z$  numbers were rounded to nearest integer for comparison. In practice, this meant that most numbers were rounded down since endogenous compounds are typically hydrogen-rich and poor in elements having large negative mass defects. The ESI/APCI/DIOS/MALDI  $m/z$  lists were then compared fractionwise with each fraction comparison represented by four columns representing APCI, ESI, DIOS, MALDI. For this the Excel formula syntax: =COUNTIF(\$A\$1:\$D\$100,A1) was used (columns A–D and 100 rows). Overlapping  $m/z$  values were removed, resulting in unique ion lists for each fraction.

## RESULTS AND DISCUSSION

**Increasing Metabolite Coverage. (I) Positive and Negative Ionization.** Separate LC–MS analyses were performed in positive and negative modes on human blood serum methanol extracts using ESI, APCI, and multimode<sup>23</sup> (MM) ionization, which is simultaneous ESI and APCI ionization. The serum extract was analyzed in five replicate injections for each polarity and ionization method. All the raw data were processed in the same analysis batch for peak finding, grouping, and retention time alignment using the XCMS software.<sup>25</sup> After initial processing including deisotoping of ion feature lists, ions unique to either “positive” or “negative” mode polarity data were identified. These are ions where “a specific  $m/z$  ( $[\text{M} + \text{H}]^+$  or  $[\text{M} + \text{Na}]^+$ ) detected at a specific retention time for which there is no corresponding negative ion ( $[\text{M} - \text{H}]^-$ ) of the ion detected at the same retention time in negative mode”. A unique ion feature in negative mode was defined as “a certain  $m/z$  ( $[\text{M} - \text{H}]^-$ ) detected at a specific retention time for which there is no ion corresponding to  $[\text{M} + \text{H}]^+$  or  $[\text{M} + \text{Na}]^+$  of the particular ion detected at the same retention time in positive mode”. The results are displayed in Table 1. For each of the investigated ionization methods, >90% of the ions detected in a particular polarity mode were found to be unique to that particular polarity when compared to the opposite polarity of the same ionization method. As the entire data set was evaluated, three categories of ions emerged: (1) Ions with corresponding ions detected in opposite polarity as illustrated with the spectra at 13.8 min in Figure 1. (2) Ion features for which different in-source fragmentation cannot be excluded and, hence, potentially only unique in a molecular ion sense. This category is illustrated in the spectra at 29.7 min in Figure 1. The feature at  $m/z$  496  $[\text{M}]^+$  (29.7 min, Figure 1) was previously identified as palmitoylglycerophosphatidylcholine in serum<sup>15</sup> and in negative ion mode palmitic acid  $[\text{M} - \text{H}]^-$  is putatively identified at  $m/z$  255. However, it cannot be excluded that the palmitoylglycerophosphatidyl backbone contributes through coelution to the base peak at  $m/z$  255 via formation of the carboxylate anion.<sup>26</sup> (3) Ion features that are truly unique to a particular polarity as illustrated with the negative ion at  $m/z$  311 tentatively identified as arachidonic acid at 32.5 min in Figure 1. The unique ion data presented in Table 1 represent ions from mainly category 3, but the potential presence of ions from category 2 cannot be excluded, thereby leading to an overestimation of the number of unique ions. Acquisition of MS data in both (+) and (–) modes in a

(26) Murphy, R. C. *Mass Spectrometry of Phospholipids: Tables of Molecular and Product Ions*; Illuminati Press: Denver, CO, 2002.

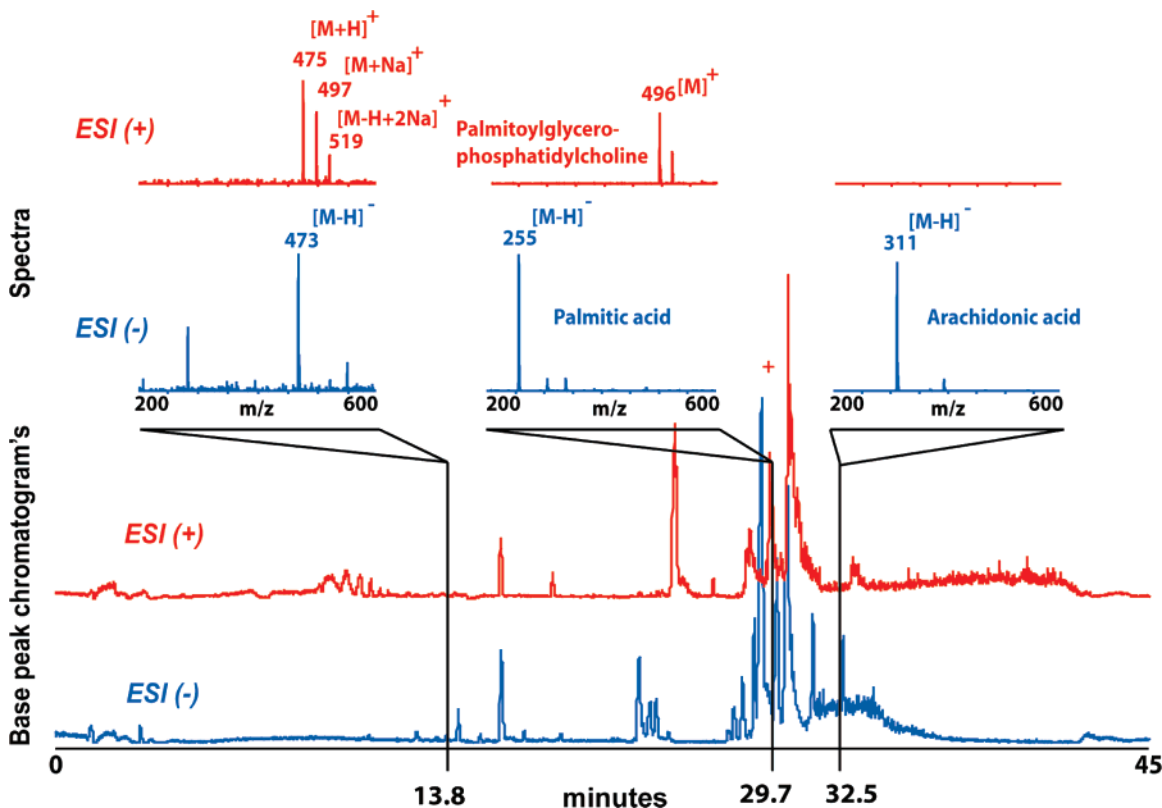


**Figure 1.** Representative examples of ion features found to be unique or shared in ESI when time slices of the TICs of positive (+) and negative (-) ionization were compared. At 13.8 min is an example of a metabolite that ionizes both in (+) mode as  $[M + H]^+$  and  $[M + Na]^+$  and  $[M + 2Na]^+$ , and in (-) mode is detected as  $[M - H]^-$ . At 29.7 min in (+) mode, the  $[M]^+$  of a palmitoylglycerophosphatidylcholine is detected whereas at the same retention time in (-) mode, the  $[M - H]^-$  of a fatty acid (palmitic acid) is observed. Finally, at 32.5 min, the  $[M - H]^-$  of a fatty acid (tentatively identified as arachidonic acid) is detected with no ions being recorded in the (+) ESI mode.

metabolomics context is previously reported,<sup>16,17,19,27,28</sup> but to our knowledge, the extent of information gain in terms of unique ions has never previously been quantified. It would be interesting to evaluate high-resolution/high-accuracy metabolomics mass spectrometry data for a number of unique ions in (+) and (-) analysis mode since the distinction of unique ions could be more precise.

**(II) Combination of "Inline" Atmospheric Pressure Ionization Methods.** The deisotoped lists of ion features from positive and negative ionization was sorted according to the presence in the respective ionization method, ESI, APCI, and MM.<sup>23</sup> A threshold for each feature of being present in one of five replicates was used. From this list with the presence/no presence of the ion features in the different ionization modes, a Venn diagram was generated (Figure 2a). The MM ionization feature is a compromise between ESI and APCI, and subsequently, the outcome of this comparison is sensitive to the MM ionization parameters. The 22 ion features assigned as unique to MM were actually also found in ESI when raw data were examined, but at an intensity level below the threshold used for XCMS peak finding. By changing ionization parameters in the MM function, the ionization can be tilted toward ESI or APCI. The parameters selected in this study (vendor-recommended default parameters for MM operation) seemed to favor ionization through an ESI

mechanism slightly over an APCI ionization mechanism. In Figure 2b,c, time slices (spectra) of the total ion chromatograms (TICs) from ESI, APCI, and MM are shown to highlight spectra representing differences shown in the Venn diagram. At 17 min, prednisone, which was added to the sample as a quality standard, is detected using ESI and MM. The  $[M + H]^+$  ion of prednisone at  $m/z$  359 is detected in both ESI and MM ionization modes, but more intensely using MM. At 17 min in APCI ionization mode, three different ions dominate the spectra, which are not molecular ion or fragment ions of prednisone, thus illustrating coeluting compounds with different ionization properties. At 23 min, the sodium adduct  $[M + Na]^+$  at  $m/z$  308 of an unknown metabolite with  $[M + H]^+$  at  $m/z$  286 is detectable using ESI and MM but not APCI mode (Figure 2c). Furthermore, cholesterol was identified at 35 min in APCI and MM ionization modes, but with a significantly lower signal using simultaneous APCI and ESI ionization, reflecting the compromise in ionization conditions. With a mass accuracy of  $\sim 0.2$  amu, there is obviously potential to underestimate the unique ion assignments, since ion species appearing less than 0.2 amu apart would be combined into one species.

The use of dual ESI and APCI ionization to probe biological systems was pioneered by Byrdwell<sup>29</sup> using two separate mass spectrometers coupled to the same separation system. Furthermore, the two separate ionization methods have been combined

(27) Idborg, H.; Zamani, L.; Edlund, P. O.; Schuppe-Koistinen, I.; Jacobsson, S. *J. Chromatogr., B: Anal. Technol. Biomed. Life Sci.* **2005**, *828*, 9–13.

(28) Ullsten, S.; Danielsson, R.; Backstrom, D.; Sjoberg, P.; Bergquist, J. *J. Chromatogr., A* **2006**, *1117*, 87–93.

(29) Byrdwell, W. C. *Rapid Commun. Mass Spectrom.* **1998**, *12*, 256–272.

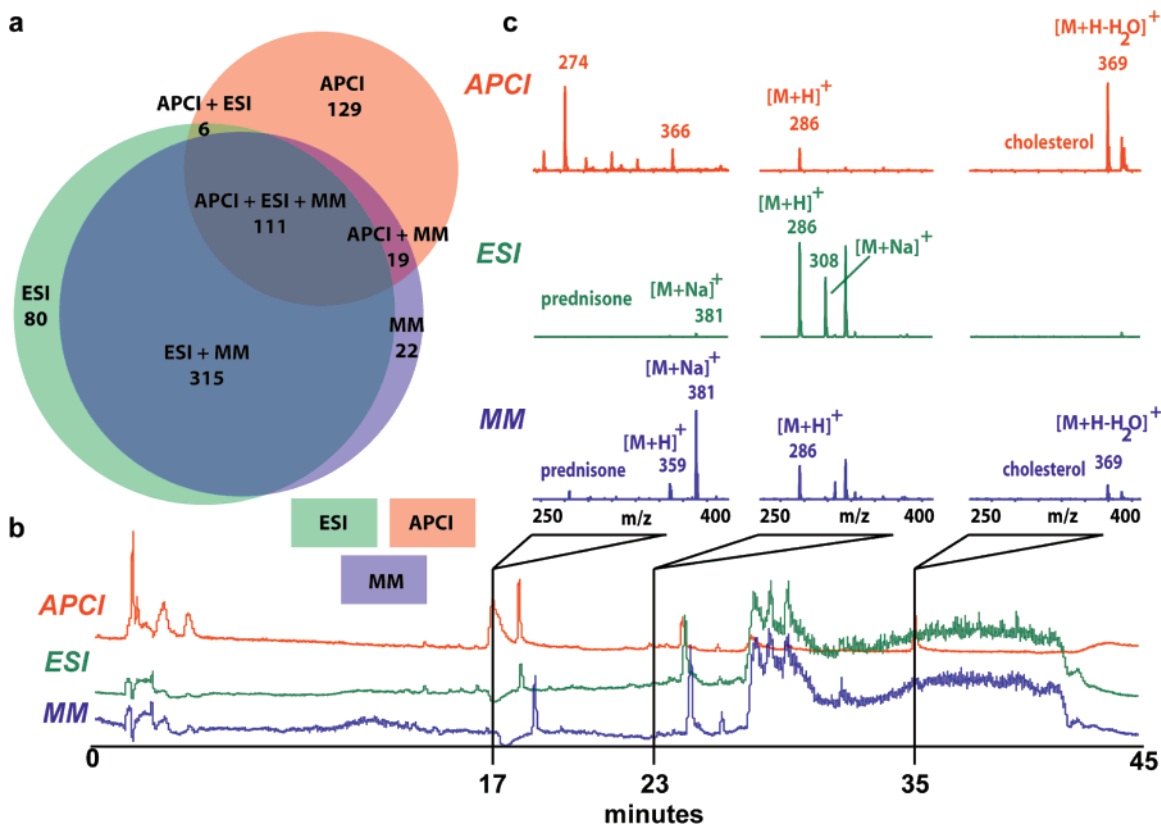


**Figure 2.** (a) Venn diagram illustrating the proportion of unique and overlapping ion features when the three different ionization methods, APCI, ESI, and MM, simultaneous APCI and ESI are compared in positive mode. (b) TICs of (+)-APCI, (+)-ESI, and (+)-MM. (c) Spectral differences at selected time slices of the TICs. At 17 min, the APCI spectra are not shown in the same scale as ESI and MM (higher intensity); spectra from 23 and 35 min are shown using the same intensity scale.

in a single source allowing for either separate or simultaneous ESI/APCI operation.<sup>30,31</sup> We used a multimode ESI/APCI source<sup>23</sup> to analyze methanol-extracted human serum. When analyzing combinatorial libraries, natural products, or drug molecules, it has been observed that ESI only ionizes ~90% of compounds.<sup>30,31</sup> Our results are consistent with this estimate showing an additional ~20% more unique ions detected using APCI for analyzing human serum. However, in extracted serum, the true proportion of metabolites not detected using ESI is most likely higher. Using MM ionization for metabolomics applications offers an advantage in terms of enhanced detection of metabolites at higher throughput since the same source (with different source parameters settings) can be used for both ESI and APCI analysis without the need of physically alternating the ionization source. However, as observed in the case of cholesterol (Figure 2c, 35 min), this might come with a slight tradeoff in sensitivity. The proportionally larger fraction of unique ions detected using APCI (129) over ESI (80) (Figure 2) reflects the fundamentally different ionization chemistry observed in an APCI source. Many of the neutral compounds lacking a basic or acidic ionizable moiety, such as NH, NH<sub>2</sub>, or COOH, will ionize only in APCI mode, whereas quite a few of the compounds possessing such a moiety will ionize in both ESI and APCI, resulting in a proportionally larger fraction of uniquely detected compounds using APCI. In fact, it is possible that the

number of unique ions in APCI could have been even larger since APCI is more of a mass-sensitive ionization than the concentration-sensitive ESI. Therefore, the APCI analysis would have benefited from a larger injected volume/higher flow rate separation system, where many of the compounds with or without functionalities such as NH, NH<sub>2</sub>, or COOH may have ionized, but instead are present at a level below their limits of detection in the current LC-APCI system.

**(III) Combined “Inline” and “Offline” Ionization.** The last level of multimode ionization was combining inline LC-APCI/ESI-(+)MS with LC fraction collection through a postcolumn T-split and subsequent offline (+)-MALDI/DIOS mass spectrometry. In Figure 3, the setup is illustrated schematically. For the ESI/APCI/MALDI/DIOS comparison, time segments in the LC-ESI/APCI data were summed and compared to the offline (from the collected fractions) acquired DIOS/MALDI spectra (Figure 3). The number of unique *m/z* values for each ionization method is shown in Figure 3. Of the unique ions detected, DIOS accounts for ~50% in each fraction, illustrating that DIOS can generate ions in the gas-phase complementary to those generated using ESI and APCI. Putative identification of unique DIOS compounds includes a disaccharide in fraction 2 and galactosylceramide sulfate in fraction 3. These identifications are based solely on the accurate mass produced by the TOF instrumentation (~5–10 ppm mass error) and, hence, should be viewed as tentatively identified compounds. To our knowledge, this is the first report comparing redundant ion sets between ESI and offline DIOS mass spectrometry.

(30) Siegel, M. M.; Tabei, K.; Lambert, F.; Candela, L.; Zoltan, B. *J. Am. Soc. Mass Spectrom.* **1998**, *9*, 1196–1203.

(31) Gallagher, R. T.; Balogh, M. P.; Davey, P.; Jackson, M. R.; Sinclair, L.; Southern, L. *J. Anal. Chem.* **2003**, *75*, 973–977.

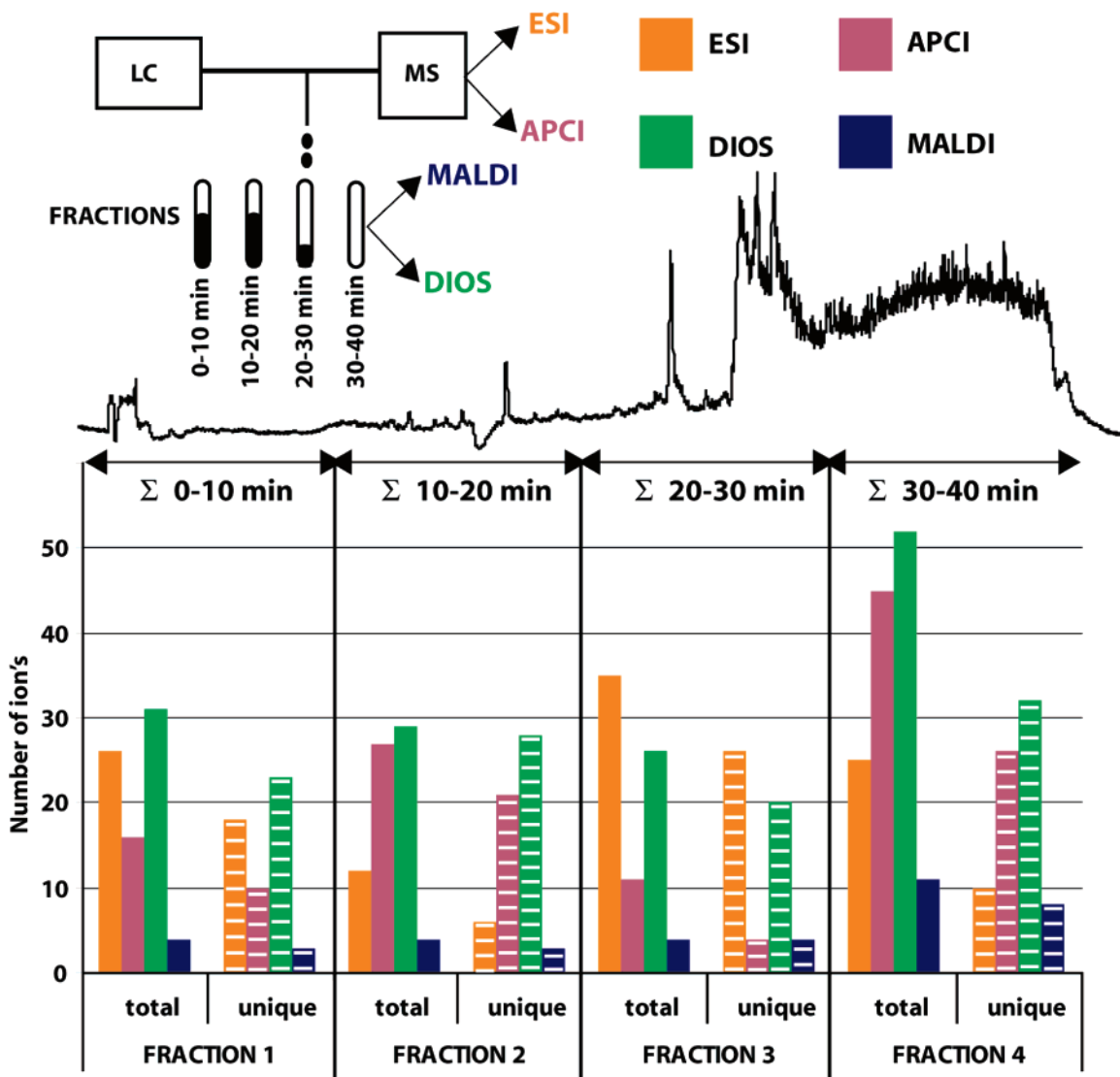


**Figure 3.** Four elution fractions collected during the LC-ESI/APCI experiments. These fractions were subsequently analyzed using DIOS and MALDI. Bar graph illustrates the total number of ions detected (solid bars) and unique ions (dashed bars) when comparing summarized ESI and APCI spectra with DIOS and MALDI spectra for overlapping ions.

In metabolomics, valid quantitative results are important and so the quantitative aspect of the offline measurement was validated using calibration curves in two different concentration ranges (Table 2). Stable isotope-labeled phenylalanine ( $^2\text{H}_5$ ) was used as internal standard for four different model compounds, phenylalanine, caffeine, cholesterol, and maltotriose. The data were averaged over three spots and three acquired spectra for each concentration in the calibration curve. Unlabeled phenylalanine displayed good linearity in both concentration ranges. The other compounds did not produce as good regression coefficients in the calibration curves but were still within acceptable limits for at least mining larger concentration differences, and there was no appreciable difference in response linearity between MALDI and DIOS. Ionization suppression effects due to multiple analytes, concentration span among analytes, or solvent/additives are well-known and characterized in ESI,<sup>32,33</sup> in APCI,<sup>34</sup> and in MALDI,<sup>35,36</sup>

and it can be assumed that they constitute an issue for DIOS as well. The best strategy to compensate for suppression is to add a stable isotope-labeled standard of the analyte of interest. However, in metabolomics, where the aim is to measure all metabolites in a biological system, the addition of possibly hundreds of analyte standards would cause further suppression problems. Adding a set of labeled standards representing the various analyte groups that can be suspected to be present in the system that is studied is most likely the best compromise and has been chosen in other studies<sup>1,13</sup> using other ionization methods.

If both time and sample are available, our result demonstrates that both ESI/APCI and offline MALDI/DIOS ionization (Figure 3) allow for the most comprehensive metabolite coverage. It is quite possible that some ions assigned uniquely to DIOS actually ionize in ESI or APCI but that they are present below the detection

(32) Niessen, W. M. A.; Manini, P.; Andreoli, R. *Mass Spectrom. Rev.* **2006**, *25*, 881–899.

(33) Cech, N. B.; Enke, C. G. *Mass Spectrom. Rev.* **2001**, *20*, 362–387.

(34) Sangster, T.; Spence, M.; Sinclair, P.; Payne, R.; Smith, C. *Rapid Commun. Mass Spectrom.* **2004**, *18*, 1361–1364.

(35) Baumgart, S.; Lindner, Y.; Kuhne, R.; Oberemm, A.; Wenschuh, H.; Krause, E. *Rapid Commun. Mass Spectrom.* **2004**, *18*, 863–868.

(36) Wang, M. Z.; Fitzgerald, M. C. *Anal. Chem.* **2001**, *73*, 625–631.



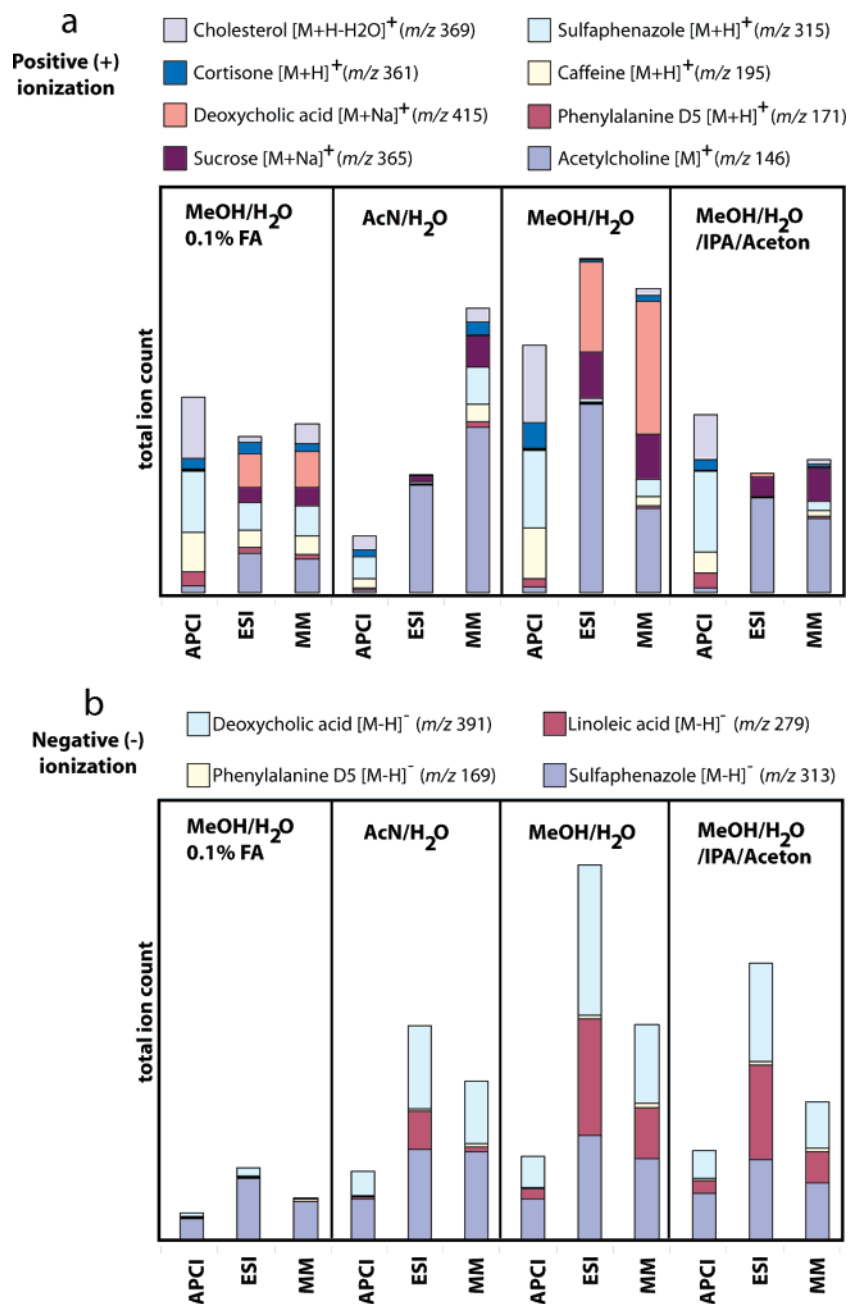


**Figure 4.** (a) Total ion count in positive polarity mass spectrometry for APCI, ESI, and simultaneous APCI and ESI ionization (MM). Intensities were obtained from summed spectra after infusion of standard mixture dissolved in the different solvent mixtures over 30 s. (b) Same as in (a) but using negative polarity ionization mode.

limit of the mass detector. Previous DIOS work has pointed toward extremely low detection limits,  $\sim 800$  ymol,<sup>37</sup> suggesting that the superior detection limit using DIOS might account for many of the uniquely detected ions.

Combining GC/ and LC/MS data for metabolomics is also a straightforward way to increase metabolite coverage.<sup>38</sup> The rationale for not including GC/MS in the present study was to achieve easily comparable spectral data for quantification of redundant and unique ions between the compared ionization techniques. Whereas ESI, APCI, DIOS, and MALDI primarily

generates adduct ions ( $[M + H]^+$ ,  $[M + Na]^+$ ,  $[M + K]^+$ ) with little or no fragmentation, GC/MS (with EI) generates little or no molecular ion and extensive fragmentation, making it difficult to compare spectral information with other ionization techniques. However, extensive compound EI spectral libraries available make GC/MS a very potent method for metabolomics since metabolites thus can be more easily identified. Derivatization before LC–MS analysis is another strategy for increasing analyte sensitivity toward ionization.<sup>39,40</sup>

**Solvent System Selection.** To be able to directly compare data sets and identify unique ions, it was important that metabolite elution order remained the same. Therefore, an important aspect was to find a preliminary compromise in the choice of solvents

(37) Trauger, S. A.; Go, E. P.; Shen, Z. X.; Apon, J. V.; Compton, B. J.; Bouvier, E. S. P.; Finn, M. G.; Siuzdak, G. *Anal. Chem.* **2004**, *76*, 4484–4489.

(38) Broeckling, C. D.; Huhman, D. V.; Farag, M. A.; Smith, J. T.; May, G. D.; Mendes, P.; Dixon, R. A.; Sumner, L. W. *J. Exp. Bot.* **2005**, *56*, 323–336.



with respect to retention and ionization efficiency, thus providing means of using the same solvent system for all of the ionization modes evaluated. In order to determine the optimal solvent system, a set of standards, cholesterol, cortisone, deoxycholic acid, sucrose, sulfaphenazole, caffeine, phenylalanine, acetylcholine, and linoleic acid representing different physical–chemical properties was dissolved in four different carrier solvents, namely, methanol/water/formic acid (49.95:49.95:0.1), acetonitrile/water (50:50), methanol/water (50:50), and methanol/water/2-propanol/acetone (25:50:12.5:12.5) and infused into the mass spectrometer. The three different ionization methods, ESI, APCI, and MM<sup>23</sup> ionization, were evaluated in both the positive and negative modes. The results are shown in Figure 4. As expected, the choice of solvent affected the observed signal for the different compounds to a different extent. Addition of 0.1% formic acid resulted in an even intensity distribution of investigated compounds in the positive ion spectra (Figure 4a). However, strong suppression of ions in negative ion spectra was observed using this solvent system (Figure 4b); this excludes addition of acid to a solvent system intended to be used in both positive and negative ion modes. For successful APCI ionization, the analytes must have higher proton affinity than the involved solvents (in positive ion mode). Acetonitrile has a higher proton affinity than water and methanol (779 versus 691 and 754 kJ/mol, respectively) and will consequently act as a proton scavenger resulting in less analyte ion formation. It was confirmed that acetonitrile suppressed ion formation of tested compounds in positive ion mode (Figure 4a). While the overall highest ion intensities were observed with methanol, the addition of acetone and 2-propanol to the methanol also gave good ion intensity distribution and resulted in improved chromatographic peak shapes compared to methanol only (data not shown).

(39) Nordstrom, A.; Tarkowski, P.; Tarkowska, D.; Dolezal, K.; Astot, C.; Sandberg, G.; Moritz, T. *Anal. Chem.* **2004**, *76*, 2869–2877.

(40) Halket, J. M.; Waterman, D.; Przyborowska, A. M.; Patel, R. K. P.; Fraser, P. D.; Bramley, P. M. *J. Exp. Bot.* **2005**, *56*, 219–243.

## CONCLUSIONS

We have quantified how the information content produced by mass spectrometry-based metabolomics can be increased by a multiple mode ionization strategy. For extracted serum analyzed with ESI in positive mode, ~90% more ions were detected by also performing analysis in the negative mode. Complementing the (+)-ESI analysis with (+)-APCI resulted in an additional ~20% increase in number of detected ions. Finally, by combining inline (+)-ESI with (+)-APCI and offline (+)-MALDI/DIOS analysis, the information content more than doubled compared to ESI only.

Changes in the metabolome are the ultimate downstream effect of altered proteome properties and gene transcription and therefore represent a principle element of global systems biology. In order to create this global view of the metabolome, analytical strategies (metabolomics) are needed to meet sample availability and throughput demands with the ambition of gaining a comprehensive metabolite profile. The data presented in this work reveal how metabolite information can be influenced and optimized through careful consideration of ionization approaches used in mass spectrometry based metabolomics.

## ACKNOWLEDGMENT

This work was funded by DOE grant DE-FG02-07ER64325 and NIH grant P30 MH062261-07. A.N. is supported by a postdoctoral fellowship from The Swedish Research Council (VR). The authors acknowledge Dr. Tim Hulsen for providing the Venn diagram resource at (<http://www.venndiagram.tk>).

Received for review August 15, 2007. Accepted October 25, 2007.

AC701982E